PRAMANA
— journal of
physics

Vol. 66, No. 1
January 2006
pp. 251–259

Anomalous density of states in hybrid normal metal–superconductor bilayers

A K GUPTA[1,*], L CRÉTINON[2], B PANNETIER[2] and H COURTOIS[2]
[1]Department of Physics, Indian Institute of Technology Kanpur, Kanpur 208 016, India
[2]Centre de Recherches sur les Très Basses Températures - C.N.R.S. associé à l'Université Joseph Fourier, 25 Avenue des Martyrs, 38042 Grenoble, France
[*]E-mail: anjankg@iitk.ac.in

Abstract. In contact with a superconductor, the Andreev reflection of the electrons locally modifies the N metal electronic properties, including the local density of states (LDOS). We investigated the LDOS in superconductor–normal metal (Nb–Au) bilayers using a very low temperature (60 mK) STM on the normal metal side. High resolution tunneling spectra measured on the Au surface show a clear proximity effect with an energy gap of reduced amplitude compared to the bulk Nb gap. The dependence of this mini-gap width with the normal metal thickness is discussed in terms of the Thouless energy. Within the mini-gap, the density of states does not reach zero and shows clear sub-gap features. We compare the experimental spectra with the well-established quasi-classical theory.

Keywords. Proximity effect; density of states; Andreev reflection.

PACS Nos 74.45.+c; 68.37.Ef; 73.40.Gk; 74.78.Fk

1. Introduction

A superconductor (S) can locally induce superconducting properties into a normal metal (N) coupled to it due to the proximity effect. The characteristic energy scale of this proximity superconductivity is not the bulk superconductor energy gap but given by $\hbar/\tau_{\rm AR}$, where $\tau_{\rm AR}$ is the time taken to traverse the normal metal thickness (L_n). In the clean limit $\tau_{\rm AR} \simeq L_n/v_{\rm F}$ [1] and the electronic density of states has features at the energy scale given by $\hbar v_{\rm F}/L_n$ and in the diffusive limit, $\tau_{\rm AR}$ is the diffusion time ($\tau_{\rm D} \simeq L_n^2/D$), with D being the diffusion coefficient of the normal metal. In the latter case if normal metal has a finite thickness (L_n), it is predicted to have a true energy gap [2] in the density of states given by

$$E_{\rm g} \simeq \frac{\hbar D}{L_n^2}. \tag{1}$$

This energy scale (also known as the Thouless energy) is well-known in the field of mesoscopic physics as it appears in the spectral rigidity and persistent currents [3].

One of the goals of the present experiment is to verify that the gap is indeed given by the Thouless energy in a simple bilayer geometry.

To get a physical understanding of this proximity superconductivity, one has to consider the microscopic mechanism of the Andreev reflection at the N–S interface [4]. An electron arriving on the interface from the normal metal side cannot find any state in the superconductor if its energy lies within the energy gap of the superconductor. The only way it can enter the superconductor is by forming an electron pair with another electron from the normal metal. A Cooper pair is then transferred in the superconductor and a hole gets retro-reflected into the normal metal. The incident electron and reflected hole phases are correlated and coupled to the superconducting condensate phase [5]. This Andreev process does not involve any energy transfer from one side to the other. The phase correlation of an Andreev pair does not involve any attraction between electrons in the normal metal, and it occurs only because of a boundary condition at the N–S interface. This energy-dependent phase change on Andreev reflection and the phase evolution during τ_{D} (the travel time of an electron or hole through the thickness of the normal metal) give rise to a constructive or destructive interference. The constructive interference criterion decides the energies at which one will find electronic states in the normal metal side and hence the density of states.

As compared to the transport experiments, local density of states measurement has a strong advantage as it probes the local information that is not averaged over the full sample area. The energy dependence of the local density of states also brings an exhaustive information on the phase-coherent coupling of electron states to the superconducting interface. The prediction is that the local density of states should show a fully opened gap (a mini-gap) in the case of a closed normal metal system [2,6,7]. Indeed, in a closed system, every electronic trajectory will couple to the superconducting interface. This will be the case of a normal metal of finite length, in practice smaller than the phase-breaking length.

The local density of states in the vicinity of a N–S junction has been measured with the help of submicron planar tunnel junctions [8]. The appearance of a pseudo-gap in the N metal as well as the inverse proximity effect on the S metal side [9] were observed. A good agreement with the quasi-classical theory based on the Usadel equations [2] and with the Bogoliubov–de Gennes equations [10] was obtained. A local study is welcome in order to overcome the unavoidable spatial averaging of such conventional experiments. Indeed, the scanning tunneling microscopy (STM) in the spectroscopy mode enables one to measure the very local density of states under the tip. Due to the technical complexity of (very) low-temperature STM, the local study of mesoscopic superconductors is still in its infancy. Inoue and Takayanagi [11] measured the tunneling spectra of a Nb–InAs–Nb system at 4.2 K. Pioneering work by Tessmer *et al* [12] focused on the proximity effect in Au nano-sized islands on top of a $NbSe_2$ sample. Levi *et al* [13] studied complex Ni–Cu–NbTi multifilamentary superconducting wires. Recently, a $NbSe_2$ crystal covered with Au [14] was also investigated. Vinet *et al* [15] performed low-temperature spatially-resolved spectroscopy of Nb–Au structures patterned by lithography.

2. Experiment

In this paper, we review our recent experiments with the goal to test the evolution of the mini-gap width with the normal metal thickness (L_n). With this objective, we fabricated a series of N–S bilayers with a fixed S thickness and a varying N thickness. To our surprise, we discovered new features that appear in addition to the expected mini-gap. The main effect is the appearance of a non-zero density of states within the mini-gap energy window.

We fabricated simultaneously a series of Nb–Au bilayers, with a fixed Nb thickness and varying Au thickness, on a single (size: $6 \times 40 \times 0.5$ mm^3) Si substrate strip. The Nb layer thickness was chosen to be significantly larger than the superconducting coherence length in order to avoid any effect due to the finite thickness of the superconductor. For varying Au thickness, another Si wafer was used as a mask and moved *in situ* above the Si substrate. After depositing the 120 nm Nb film, the Au film (from 10 to 260 nm) was deposited within 15 min at a pressure below 10^{-8} mbar. These conditions minimize the interface contamination and should preserve the best Nb–Au interface transparency. The full Si wafer with the bilayer films thus obtained (see figure 1a) was cleaved in air to separate different samples. Individual Au (260 nm) and Nb (120 nm) layers were characterized by transport measurements as summarized in table 1, together with calculated values for the characteristic length scales:

$$\xi_{n,s} = \sqrt{\frac{\hbar D_{n,s}}{2\Delta}}. \tag{2}$$

Each bilayer sample was cooled separately in an STM working at 60 mK [16]. A fresh-cut Pt–Ir wire was used as the STM tip. A STM image of the 72 nm Au sample at very low temperature (100 mK) is shown in figure 1b. We observe a polycrystalline structure with a grain size of about 50 nm, which is consistent with the measured elastic mean free path $l_{e,n}$ of 36.1 nm. The rms surface roughness is 3.4 nm. Thus our Au films are clearly in the diffusive regime, except for the smaller

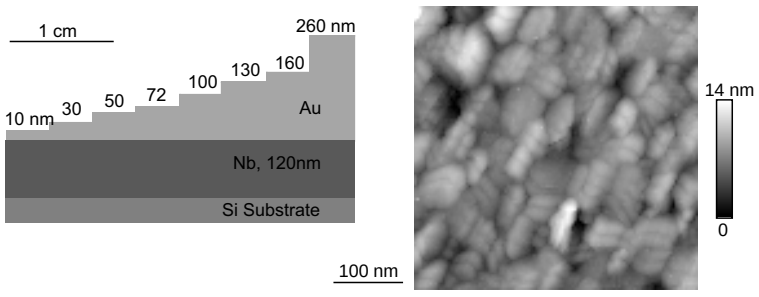

(a) (b)

Figure 1. (**a**) Schematic cross-section of the full Nb–Au bilayer sample. (**b**) STM image (410×410 nm^2) at 100 mK of the sample with a Au thickness of 72 nm. The rms roughness for this sample from this image is found to be 3.4 nm.

Table 1. Transport properties of the Nb (120 nm) and Au (260 nm) films at 10 K. The RRR is the ratio of the room-temperature resistivity with the residual resistivity (at 10 K).

	ρ ($\mu\Omega$ cm)	RRR	l_e (nm)	D (cm^2/s)	ξ (nm)
Nb	16.2	3.7	5.4	24.7	23.2
Au	2.34	4.7	36.1	169	60.8

thicknesses where ballistic effects may occur. On every sample, we acquired a series of $I(V)$ tunnel spectra, at a tunnel resistance of 5 to 12 MΩ, and at numerous places in order to check reproducibility. The acquired spectra were actually reproducible over the sample surface with minor variations, and also point-like defects at a few locations. The $I(V)$ data were numerically differentiated to obtain the differential conductance $\mathrm{d}I/\mathrm{d}V(V)$, which gives the LDOS at the energy eV with a resolution limited by the thermal smearing. A selection of the tunneling spectra is shown in figure 2. The spectra are flat at large bias voltages ($|V| \gg 2.5$ meV) and have been normalized to make this conductance value as 1.

For the bilayer with the smallest Au thickness (10 nm), the spectrum qualitatively resembles a BCS spectrum with a gap amplitude very close to the expected bulk Nb gap: $\Delta/e \sim 1.5$ meV. For larger thicknesses, the spectra show a mini-gap that reduces in width with increasing Au thickness. There seems to be a cross-over from one type of spectra to another at Au thickness between 72 and 100 nm. For small thicknesses, there is a sharp rise to a peak in the LDOS at Δ/e, and a relatively slow decrease as we go towards zero bias. For large thicknesses, there is a small

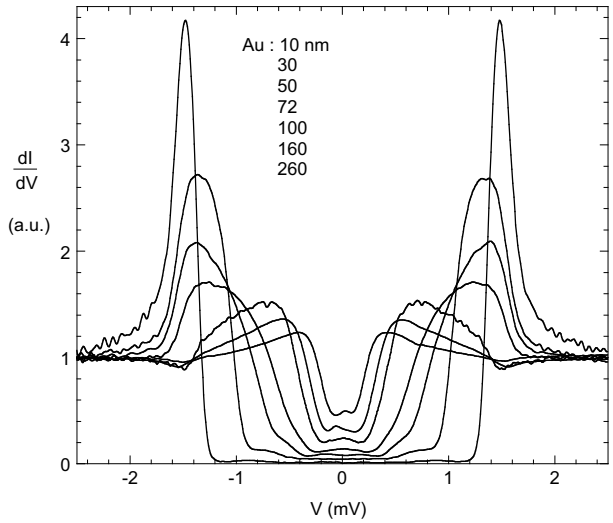

Figure 2. Tunneling density of states measured at 60 mK at the Au surface of Nb–Au bilayer samples with a varying Au thickness L_n. Data from the 130 and 200 nm samples are not shown for ease of reading.

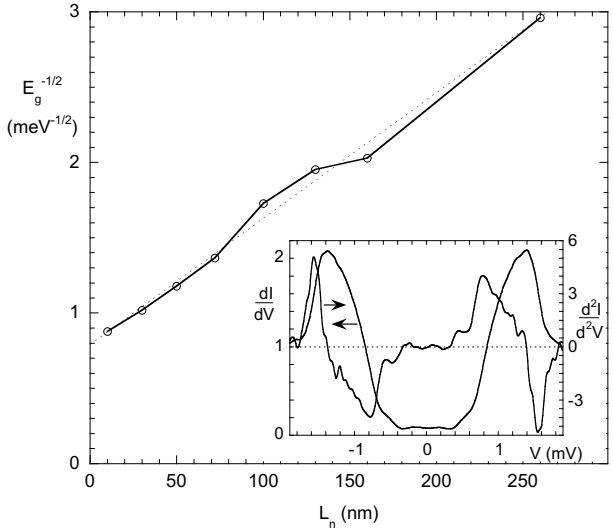

Figure 3. Variation of the quantity $E_{\rm g}^{-1/2}$, the mini-gap $E_{\rm g}$ being defined in the inset by the inflection point in $\mathrm{d}I/\mathrm{d}V(V)$, with the N metal length L_n. The dashed line shows the best fit mini-gap as described by eq. (3). Inset: Tunneling spectra of the 50 nm sample together with its derivative $\mathrm{d}^2I/\mathrm{d}V^2$.

dip at Δ/e, the LDOS then rises slowly to a peak and falls off rapidly inside the mini-gap. This dip feature at Δ actually implies that the superconducting gap in the bulk of Nb is not significantly influenced by a large thickness of Au.

From the experimental tunneling spectra, we extracted the energy gap $E_{\rm g}$ as the energy at the inflection point, i.e. with a maximum slope $\mathrm{d}^2I/\mathrm{d}V^2$. The quantity $E_{\rm g}^{-1/2}$ is plotted in figure 3 as a function of the N metal length L_n, so that a Thouless energy scaling should appear as a linear behavior. The best fit of $E_{\rm g}^{-1/2}$ vs. L_n gives the expression:

$$E_{\rm g} = \frac{1.43{\times}10^4}{(94.7 + L_n)^2}\ \text{meV}, \tag{3}$$

L_n being in nm units. As naively expected from table 1, the numerator value is of the order of $\hbar D_n = 1.09 \times 10^4$ meV·nm^2. The extra length appearing in the denominator expresses the fact that the Andreev reflection happens in the superconductor over this length scale, which also makes $E_{\rm g}$ extrapolate to Δ as L_n goes to zero.

Inside the mini-gap, the density of states is strikingly different from zero and features a few sub-gap structures. The second derivative of the tunneling current with respect to the voltage $\mathrm{d}^2I/\mathrm{d}V^2$ shown in the inset of figure 3 actually displays clear step-like structures. These features do not scale with the bulk Nb energy gap Δ, as their energy position evolves with the normal metal length L_n. This effect is therefore not a ballistic one which would be restricted to the smaller thicknesses. Let us point out that the energy resolution of our STM is better than 36 μeV or

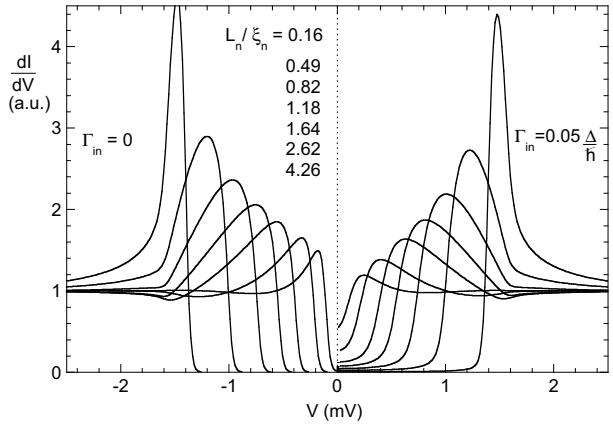

Figure 4. Calculated spectra using Usadel equations for a bilayer geometry with calculation parameters $L_s/\xi_s = 5.17$, $\Delta = 1.57$ meV, $T = 210$ mK, $\Gamma = 0.6$, $r_B = 0$, and $\xi_n = 60.8$ nm. The right part ($V < 0$) curve stands for $\Gamma_{\rm in} = 0$ and the left part ($V > 0$) curve for $\Gamma_{\rm in} = 0.05\Delta/\hbar$.

210 mK [16], which rules out thermal smearing as a cause of such a large (up to 50%) zero bias conductance.

3. Usadel solutions

We compared our data to the predictions of the quasi-classical theory in the diffusive regime [6,17], by solving the Usadel equations with the help of a numerical code from Belzig *et al* [2]. The input parameters for this calculation are the lengths $L_{n,s}$ of N and S metals in units of the related coherence lengths $\xi_{n,s}$, the electronic properties mismatch parameter

$$\Gamma = \frac{\rho_s \xi_s}{\rho_n \xi_n} \propto \sqrt{\frac{l_{e,n}}{l_{e,s}}}, \tag{4}$$

the specific interface resistance r_B, the inelastic $\Gamma_{\rm in}$ and spin-flip $\Gamma_{\rm sf}$ scattering rates in the N and S metals. Here $\rho_{n,s}$ is the normal-state resistivity in N or S. We considered the interface transparency as perfect and we took into account a thermal smearing with an effective temperature of 210 mK.

We adjusted the calculation parameters to fit the tunneling spectra. Figure 4 displays two sets of calculated curves. In order to recover the observed LDOS peak amplitude and position, we had to assume a mismatch parameter Γ of value 0.6 instead of 2.6 as estimated from the transport measurements, keeping the other parameters matching precisely with the measured values. This discrepancy may be related to the Nb–Au interface roughness which is expected to affect the Andreev reflection rate, and thus the induced superconductivity in the Au layer [18].

We first assumed that the inelastic and spin-flip scattering lengths are much larger than the Au layer thickness, so that we can neglect these scattering processes. The

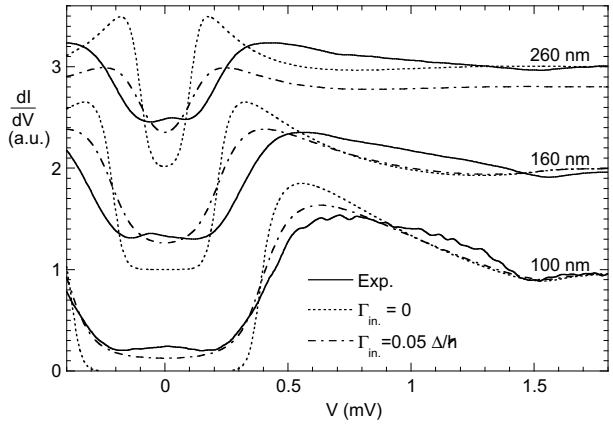

Figure 5. Comparison of the experimental data for L_n= 100, 160 and 260 nm (full line) with the calculated spectra. The calculation parameters are $L_s/\xi_s = 5.17$, $\Delta = 1.57$ meV, $T = 210$ mK, $\Gamma = 0.6$, $r_B = 0$, and $\xi_n = 60.8$ nm. The dotted line curve stands for $\Gamma_{\rm in} = 0$ and the dashed line curve for $\Gamma_{\rm in} = 0.05\Delta/\hbar$. The curves have been evenly shifted for clarity.

overall spectral shapes are qualitatively reproduced, except for the peak of the 50 nm spectra which is noticeably different from the experimental data. At large L_n, the predicted mini-gap is clearly smaller than in the experiment. Changing the $\xi_{n,s}$ values or introducing a small interface resistance in the calculation did not improve the fit. We tried to take into account the dependence of the elastic mean free path with the normal metal thickness L_n [19], and hence the related variation of the characteristic length ξ_n and of the mismatch parameter Γ with L_n. This modified the calculated spectra in the regime $L_n < 100$ nm only slightly. Obviously, we always obtain a fully opened gap with a zero LDOS at the Fermi level. This is in clear disagreement with our experimental results, where we always get a non-zero conductance at zero bias.

With the hope to obtain a better fit, we included a non-zero inelastic scattering rate in the calculation parameters. We achieved a good agreement of the calculated LDOS at the Fermi level with the measured one by choosing $\Gamma_{\rm in} = 0.05\Delta/\hbar$. This value corresponds to an inelastic mean free path of about 370 nm, which is significantly smaller than the expected value of about 2 μm. The calculated mini-gap width is unchanged and remains smaller than the experimental value. Moreover, the fit does not describe the sharpness of the sub-gap features (see figure 5). Whereas the agreement remains approximate at intermediate and small thicknesses ($L_n \leq$ 100 nm), the discrepancies are especially clear at large thickness (260 nm). We also tried to include a spin-flip scattering [8,15], but it did not improve the fit.

4. Concluding remarks

In terms of electron trajectories, a finite LDOS at the Fermi level signifies that a significant fraction of the electron states present at the Au surface do not Andreev-reflect at the Nb–Au interface on the time-scale of the phase coherence time. In

the diffusive regime of relevance here, neither the angle dependence of the Andreev reflection at an imperfectly transparent N–S interface [20] nor the possible presence of surface electron states [21] should play a role.

Our observations are somewhat reminiscent of a previous STM spectroscopy study on a small (20 nm) and presumably quite-disordered Au droplet in contact with a Nb electrode [15], where a clear filling of the LDOS at the Fermi level was also observed, in the absence of any mini-gap width evolution. Let us point out that both this and our systems are far from the strongly disordered regime where a non-zero LDOS for all energies is predicted [22]. Rather, our films have the typical polycrystalline structure of a weakly disordered thin films. The elastic diffusion in the N metal is not homogenous like in an amorphous metal but controlled by the interfaces between ballistic grains. The possible confinement of electron states within a grain can have serious effects on the LDOS in the proximity superconductivity regime which is of interest here. A significant fraction of electron states may be sufficiently decoupled from the N–S interface to avoid any Andreev reflection, thus remaining insensitive to the superconductivity in the S layer and contributes fully to the LDOS.

In conclusion, we investigated with a high energy resolution the LDOS at the N metal surface of S–N (Nb–Au) bilayers and compared it with the theoretical predictions. We uncovered a non-zero LDOS near the Fermi level that increases as the N metal thickness is increased. The same behavior is observed at small thickness when the interface transparency is reduced on purpose. This new effect cannot be described within the well-established quasi-classical theory. We suggest that the granular structure of the Au layer enables the decoupling of some electron states from the Andreev reflection at the interface, which results in a non-zero LDOS inside the mini-gap.

Acknowledgement

We thank W Belzig for sharing his numerical code and discussions, Norbert Moussy for his contribution to the early stages of this work and we acknowledge discussions with M Feigelman.

References

[1] D Saint James, *J. de Physique* **25**, 899 (1964)
[2] W Belzig, C Bruder and G Schön, *Phys. Rev.* **B54**, 9443 (1996)
[3] Y Imry, *Introduction to mesoscopic physics* (Oxford University Press, 1997)
[4] A F Andreev, *Sov. Phys. JETP* **19**, 1228 (1964)
[5] C W J Beenakker, cond-mat/9909293
[6] A A Golubov and M Yu Kupriyanov, *J. Low. Temp. Phys.* **61**, 83 (1988)
[7] F Zhou, P Charlat, B Spivak and B Pannetier, *J. Low Temp. Phys.* **110**, 841 (1998)
[8] S Guéron, H Pothier, N O Birge, D Estève and M H Devoret, *Phys. Rev. Lett.* **77**, 3025 (1996)
[9] M Sillanpaä, T Heikkilä, R K Lindell and P J Hakonen, cond-mat/0102367
[10] K Halterman and O T Valls, *Phys. Rev.* **B66**, 224516 (2002)

[11] K Inoue and H Takayanagi, *Phys. Rev.* **B43**, 6214 (1991)
[12] S H Tessmer, M B Tarlie, D J van Harlingen, D L Maslov and P M Goldbart, *Phys. Rev. Lett.* **77**, 924 (1996)
[13] Y Levi, O Millo, N D Rizzo, D E Prober and L R Motowidlo, *Phys. Rev.* **B58**, 15128 (1998)
[14] A D Truscott, R C Dynes and L F Schneemeyer, *Phys. Rev. Lett.* **83**, 1014 (1999)
[15] M Vinet, C Chapelier and F Lefloch, *Phys. Rev.* **B63**, 165420 (2001)
[16] N Moussy, H Courtois and B Pannetier, *Rev. Sci. Instrum.* **72**, 128 (2001)
[17] W Belzig, F K Wilhelm, C Bruder, G Schön and A D Zaikin, *Superlatt. Microstruct.* **25**, 1251 (1999)
[18] S Pilgram, W Belzig and C Bruder, *Phys. Rev.* **B62**, 12462 (2000)
[19] K Fuchs, *Proc. Cambridge Philos. Soc.* **11**, 1120 (1938)
[20] N A Mortensen, K Flensberg and A-P Jauho, *Phys. Rev.* **B59**, 10176 (1999)
[21] M P Everson, R C Jaklevic and Weidian Shen, *J. Vac. Sci. Technol.* **A8**, 3662 (1990)
[22] P M Ostrovsky, M A Skvortsov and M V Feigelman, *Phys. Rev. Lett.* **87**, 027002 (2001)